

Free-Radical Polymerization of Methacrylic Acid: From Batch to Continuous Using Stirred Tank Reactors

Juri Ilare^{1,#}, Nicolò Manfredini^{1,#}, Mattia Sponchioni^{1,}, Giuseppe Storti¹ and Davide Moscatelli¹*

¹ Department of Chemistry, Materials and Chemical Engineering, Politecnico di Milano, Via Mancinelli 7, 20131 Milano, Italy.

[#]JI and NM equally contributed to the work

*corresponding author: Mattia Sponchioni, e-mail: mattia.sponchioni@polimi.it

Abstract: In the last years important efforts have been made to convert the traditional batch polymer production to continuous. This transition allows to overcome most of the limitations of discontinuous or semi-continuous processes, such as environmental and safety issues and inadequate product quality. In this work we propose a model-based strategy to convert the solution free-radical polymerization of non-ionized methacrylic acid (MAA) from semibatch to continuous while preserving the product average molecular weight and polymer content. First, a purely kinetic model for the polymerization of MAA was validated for batch, semibatch and continuous stirred tank reactors (CSTR). Then, a basic optimization approach was applied to guide the transition of a selected semibatch process to a CSTR. This strategy results in a substantial productivity increase (5.1 times higher than in the original semibatch) while preserving the selected polymer average molecular weight and dry content. Finally, in order to reduce the residual monomer in the product leaving the CSTR, we simulated the addition of a tubular reactor. This was modelled introducing a small plug flow reactor in series to the CSTR. This approach represents an effective and robust tool for polymer manufacturers to assist switching their productions to continuous preserving their product portfolio.

KEYWORDS: Free-Radical Polymerization; Continuous Stirred Tank Reactor; From Batch to Continuous; Kinetic Modelling; Optimization; Poly(Methacrylic Acid)

1. Introduction

Polymers are industrially produced by means of different polymerization techniques depending upon the choice of the monomers and the desired final polymer features. Among them, one of the most important and established technique is free-radical polymerization (FRP)[1]. It can be performed either in homogeneous (*e.g.*, bulk and solution) or heterogeneous environment (*e.g.*, emulsion and

32 suspension) depending upon the monomer and polymer solubility in the continuous phase.
33 Irrespectively of the conditions, FRP can be performed in discontinuous or continuous reactors[2].
34 Nowadays, the majority of the industrial processes of polymer production relies on batch or semibatch
35 reactors, given their easy conduction and versatility of polymer grades. However, these traditional
36 configurations are characterized by safety, environment, and cost limitations. In fact, discontinuous
37 systems are typically characterized by poor productivity, mainly connected to the dead times required
38 to load the reactor, recover the product, and clean the vessel. In addition, the big volumes required by
39 the ever increasing polymer demand represent a substantial safety concern. In fact, in case of
40 disastrous situations (*e.g.*, runaway, emissions, explosions etc.) the magnitude of the related risks
41 would be extremely high. The adoption of a continuous process would allow to alleviate most of these
42 limitations. In fact, the typically high productivity of a continuous system not only enables to intensify
43 the production but also to reduce the monomer and solvent hold-up, the main source of safety and
44 environmental risks.

45 The transition from discontinuous to continuous FRP is often accomplished with difficulties, in
46 particular when the reproduction of the same process (*i.e.*, conversion, productivity, heat removal
47 capacity, etc.) and product (*i.e.*, solid content, molecular weight distribution (MWD), nanoparticle
48 size, etc.) features of the discontinuous reactor is essential. These difficulties are mainly attributed to
49 the different fluid-dynamic and residence time distribution between discontinuous and continuous
50 reactors, in addition to the difficulty in handling the viscous polymer mixture in a continuous
51 configuration. All these considerations make the transition to continuous processes in the polymer
52 field very challenging[3]–[5].

53 In this scenario, mathematical models can represent a very efficient tool to study and guide the
54 implementation of continuous processes, enabling the identification of optimal operating conditions
55 while saving time and experimental effort. For example, models have been successfully used to
56 predict the transition of the solution polymerization of non-ionized acrylic acid[6], [7] or to study the
57 impact of micromixing in the solution polymerization of methyl methacrylate (MMA) in a continuous
58 stirred tank reactor (CSTR)[8]. This is a topic of primary interest from both academic and industrial
59 points of view, as testified by several recent publications[6], [9], [10]. In particular, companies have
60 interest in the production of large volumes of polymers always preserving their quality, in order not
61 to alter their portfolio and ensure continuity in their business. In this context, one of the most
62 industrially appealing product is poly(methacrylic acid) (PMAA) mainly due to the manifold
63 applications that this polymer finds in the fields of organic coatings[11], [12], adhesives[13], [14],
64 leather treatment[15], ion-exchange resins[16], textiles[17], and paper industries[18]. Aqueous
65 solution FRP of MAA has been extensively studied in a wide range of concentrations, from 1% w/w

66 to bulk polymerization[19]–[21], but always considering batch or semibatch processes[22]–[24].
67 Indeed, to the best of our knowledge, a contribution focused on the relevant aspects of the transition
68 from the traditional discontinuous processes to the continuous ones is still missing in literature.
69 In this work, we developed a model-based strategy for the transition of a semibatch MAA production
70 to an intensified continuous process using a CSTR. In particular, we first developed and validated a
71 purely kinetic model able to predict conversion and MWD of PMAA produced either in batch,
72 semibatch or CSTR. The model was made of mass and population balance equations, with kinetic
73 parameter values as measured by pulsed laser polymerization in previous studies on MAA. Namely,
74 Lacík et al. were able to reliably estimate propagation as well as termination rate constants of MAA
75 at different concentrations and ionization degrees, providing functional forms for these constants with
76 wide range of validity [21], [25], [26]. Then, we applied this model to design the transition of a
77 selected semibatch process to a continuous one using a CSTR with the constraint of providing the
78 same weight-average molecular weight (M_w) and polymer content (PC) obtained in the semi-
79 continuous process. A basic but robust optimization approach is adopted, exploring the process
80 performances in terms of M_w , PC and productivity as a function of four different operating variables,
81 namely inlet volumetric flow rate, inlet monomer, water, and initiator concentrations. Among the
82 collected results, those providing minimum conversion of 98% and the highest productivity are
83 selected. To reduce the concentration of the residual monomer leaving the CSTR to the value imposed
84 by the current regulation, the use of a tubular reactor in series to the CSTR is finally examined.
85 With this approach, a substantial intensification of the process was achieved, while obtaining a
86 product very similar to the one produced in semibatch reactors. Therefore, this strategy could
87 represent a booster in the transition from batch to continuous polymer production.

88 **2. Experimental section**

89 **2.1. Materials**

90 Methacrylic acid (MAA, 99%), ammonium persulfate (APS, 98%), hydroquinone ($\geq 99\%$) and
91 acetonitrile (ACN, 99.9%, analytical grade) were purchased from Sigma Aldrich and used as
92 received. Analytical grade water was used without further treatment.

93 **2.2. Non-ionized methacrylic acid solution polymerization**

94 **2.2.1. Batch FRP**

95 Different polymerizations were performed using MAA as monomer, APS as initiator and water as
96 solvent. The monomer weight concentration was kept constant to 5% w/w for all the syntheses while
97 the initiator to monomer weight ratio was varied in the range 0.5-3% weight based on monomer
98 (wbm) in order to produce polymers with different molecular weights. In a typical polymerization

99 protocol, 2.5 g of MAA were solubilized in 45 g of distilled water. The solution was poured in a 100
100 mL round bottom flask equipped with a magnetic stirrer, purged with nitrogen for 30 minutes in order
101 to remove the oxygen and then heated to 50 °C in an oil bath under stirring (500 rpm). Then 0.025 g
102 of APS in 2.475 g of water were added to the flask by the use of a syringe and the reaction was let to
103 occur for 5 hours. Samples were taken at regular time intervals, hydroquinone was added to quench
104 the reaction and the conversion was evaluated via thermogravimetric analysis (described in Section
105 2.3.). For the measurements of the MWD, the samples were freeze-dried overnight using a Telstar
106 Lyoquest freeze-drier at a pressure of 0.1 mbar and -56 °C and analysed via aqueous gel permeation
107 chromatography (GPC) according to the procedure described in Section 2.4.

108 **2.2.2. Semibatch FRP**

109 These reactions were carried out varying both the initiator to monomer weight ratio and the monomer
110 feeding time (FT) in order to validate the model under different conditions. As an example, 0.23 g of
111 APS were dissolved in 49.77 g of distilled water and poured into a 100 mL round bottom flask
112 equipped with mechanical stirrer. The mixture was purged with nitrogen for 30 minutes in order to
113 remove the oxygen and placed in an oil bath at a selected temperature. In particular, for semibatch
114 reactions two different temperatures were tested, namely 50 and 60 °C. In the meanwhile, 10 g of
115 methacrylic acid were loaded in a syringe pump (New Era Pump systems, NE-300). Five different
116 FT were implemented, 20, 30, 40, 50, and 120 minutes, respectively. Once the addition of the
117 monomer was over, the polymerization was protracted in batch for further 30 minutes, in order to
118 deplete all the residual monomer. To monitor conversion and MWD during time, samples were taken
119 at regular times (*i.e.*, 0, 5, 10, 15, 25, 35, 50, 90, 120 minutes). Polymer molecular weights were
120 analysed with the protocol described in Section 2.4 while the conversion was evaluated according to
121 the procedure described in Section 2.3.

122 **2.2.3. CSTR**

123 A 100 mL round bottom flask was filled with 50 g of water. Nitrogen was bubbled for 30 minutes to
124 remove oxygen and the flask was thermostated in a pre-heated oil bath at 60 °C. The flowrates of
125 inlet and outlet streams were controlled by two peristaltic pumps (New Era Pump systems, NE-
126 9000B). In a typical experiment, an inlet stream of $5 \cdot 10^{-3}$ L/min with monomer concentration of 1.84
127 mol/L and initiator concentration of $3.97 \cdot 10^{-2}$ mol/L was fed to the reactor. The outlet volumetric
128 flow rate was adjusted in order to ensure constant reaction volume equal to 50 mL. The actual
129 experimental discretization of the outlet flowrate predicted by the model is shown in **Figure S1**.
130 Samples were taken at regular intervals in order to evaluate monomer conversion (Section 2.3) and
131 polymer MWD following the same protocol described below. In order to reach the steady state
132 conditions, the reaction experiment lasted 24 hours.

133 **2.3. Thermogravimetric analysis**

134 An Ohaus MB35 Moisture Analyser was used as already shown in literature[27]. 1 mL of the reaction
135 mixture was sampled, immediately inhibited by adding 0.06 g of hydroquinone and weighted on an
136 aluminium disk. Then, the disk was heated up to 160 °C in order to guarantee water and monomer
137 evaporation. Finally, the dry polymer was used to calculate the monomer conversion according to
138 **eqs. S1-S3 in Table S1.**

139 **2.4. MWD analysis by GPC**

140 Aqueous gel permeation chromatography analysis was performed on a Jasco 2000 system. After
141 freeze-drying the samples, they were dissolved at 5 mg mL⁻¹ in 0.05 M Na₂SO₄/acetonitrile 80/20
142 v/v solution and filtered by means of 0.45 µm pore-size nylon membrane. The flow rate was set at
143 0.5 mL min⁻¹ at the temperature of 35 °C with a guard column and three Suprema columns (Polymer
144 Standards Service; particle size 10 µm, pore sizes of 100, 1000, and 3000 Å).

145 The polymer MWD and mean values (*i.e.* weight-average molecular weight, Mw, and number-
146 average molecular weight, Mn) were evaluated by size exclusion chromatography using poly(acrylic
147 acid) (PAA) standards (16 – 1100 kDa) for the calibration curve. Therefore, the Mark-Houwink
148 equation (**eq. 1**) was applied to determine the actual (PMAA) molecular weight.

149

$$k_1 M_{P,1}^{1+a_1} = k_2 M_{P,2}^{1+a_2} \quad (1)$$

150

151 Here k and a are the Mark-Houwink parameters, which depend on the specific combination solvent-
152 polymer and temperature, M_P is the polymer molecular weight, and the subscripts 1 and 2 indicate
153 two different polymers (in our case, PAA and PMAA). Specifically, a = 0.86 and k = 0.004 mL/g and
154 a = 0.65 and k = 0.0449 mL/g were used for PAA and PMAA, respectively [28]. These values
155 correspond to temperature of 35 °C and mixed solvent at 0.05 M NaNO₃/acetonitrile 80/20 v/v, a
156 composition very similar to that of the eluent used in this work. Moreover, the same values can be
157 applied in a range of molecular weight up to 1.1 10⁶ Da, consistent with the results of this work.

158 The results provided by this analytic method, despite being reasonable for monomer conversion
159 >30%, proved to be unreliable at low polymer content. Therefore, the ability of the model to predict
160 the molecular weight distribution of the product was judged based on the data acquired at conversions
161 higher than 30% only.

162

163 **3. Model development and kinetic parameters**

164 The kinetic scheme in **Table 1** is considered. Ammonium persulfate is used as thermal initiator; given
 165 the large reactivity of the initiator fragments, the primary radicals R_1^\bullet are reported as reaction
 166 products. Active chains of any length (R_n^\bullet) undergo propagation, chain transfer to monomer and
 167 bimolecular termination, both by disproportionation and combination. Dead chains (P_n) are formed
 168 by termination reactions.

169

170 *Table 1 Kinetic scheme for the solution polymerization of non-ionized methacrylic acid: initiation (2), propagation (3), bimolecular*
 171 *termination (4), and chain transfer to monomer (5) were considered.*

Chain initiation	$I_2 \xrightarrow{k_d} 2R_1^\bullet$	$r_i = 2 \cdot f \cdot k_d \cdot I$	(2)
Propagation	$R_n^\bullet + M \xrightarrow{k_p} R_{n+1}^\bullet$	$r_p = k_p \cdot M \cdot R$	(3)
Termination by disproportionation	$R_n^\bullet + R_m^\bullet \xrightarrow{k_{td}} P_n + P_m$	$r_t = (k_{tc} + k_{td}) \cdot R^2$	(4)
Termination by combination	$R_n^\bullet + R_m^\bullet \xrightarrow{k_{tc}} P_{n+m}$		
Chain transfer to monomer	$R_n^\bullet + M \xrightarrow{k_{tr,M}} P_n + R_1^\bullet$	$r_{tr,M} = k_{tr,M} \cdot M \cdot R$	(5)

172

173 The values of all the rate constants are from the literature, mainly estimated by pulsed-laser
 174 polymerization: such values as well as the corresponding sources are summarized in **Table 2**. In case,
 175 the dependence on instantaneous monomer concentration, average chain length and reaction
 176 temperature are included. While the temperature dependence of monomer and water density is
 177 accounted for, the polymer density is assumed constant.

178

179 *Table 2 Numerical values of the parameters in the rate laws and corresponding sources.*

$k_d/(s^{-1}) = 1.17e22 \cdot \exp\left(\frac{-21169}{T/K}\right)$	[29]
$f = 0.5$	
$k_p/(L \cdot mol^{-1} \cdot s^{-1}) = 4.1e6 \cdot \exp\left(\frac{-1880}{T/K}\right) \cdot (0.08 + 0.92 \cdot \exp\left(\frac{-5.3 \cdot w_{MAA}^0 \cdot (1-X)}{1-w_{MAA}^0 \cdot X}\right) \cdot \exp(0.096 + \frac{0.11 \cdot w_{MAA}^0 \cdot (1-X)}{1-w_{MAA}^0 \cdot X}))$	[25]

$$k_t^{1,1}/L \cdot mol^{-1} \cdot s^{-1} = 2.29e12 \cdot \exp\left(\frac{-2640}{T/K}\right)$$

if $\overline{DP}_n \leq 68$:

$$k_t/(L \cdot mol^{-1} \cdot s^{-1}) = k_t^{1,1} \cdot \overline{DP}_n^{-0.61} \quad [19],$$

if $\overline{DP}_n > 68$: [30],

$$k_t/(L \cdot mol^{-1} \cdot s^{-1}) = k_t^{1,1} \cdot 68^{-0.444} \cdot \overline{DP}_n^{-0.166} \quad [31]$$

$$k_{tc}/(L \cdot mol^{-1} \cdot s^{-1}) = 0.2 \cdot k_t$$

$$k_{td}/(L \cdot mol^{-1} \cdot s^{-1}) = 0.8 \cdot k_t$$

$$C_{tr,M} = \frac{k_{tr,M}}{k_p} = 5.37 \cdot 10^{-5} \quad [19]$$

$$\rho_M/g \cdot mL^{-1} = 1.0288 - 5.5568 \cdot 10^{-4} \cdot (T/^\circ C) - 1.11132e \cdot 10^{-5} \cdot (T/^\circ C)^2 + 1.0041 \cdot 10^{-7} \cdot (T/^\circ C)^3 \quad [31]$$

$$\rho_{H_2O}/(g \cdot mL^{-1}) = 0.9999 + 2.3109 \cdot 10^{-5} \cdot (T/^\circ C) - 5.44807 \cdot 10^{-6} \cdot (T/^\circ C)^2$$

$$\rho_P/(g \cdot mL^{-1}) = 1.29 \quad [28]$$

180

181 In the table, T is the temperature, f the initiation efficiency, w_{MAA}^0 the mass fraction of MAA in
 182 solution in absence of polymer, $k_t^{1,1}$ the overall rate coefficient of bimolecular termination of two
 183 radicals of chain length one, \overline{DP}_n is the number-average chain length of the radicals, X is the
 184 conversion, ρ_M , ρ_{H_2O} and ρ_P are the monomer, water and polymer densities, respectively. The pH of
 185 the reacting mixture was carefully monitored by an Accumet AP110 meter (FisherScientific). Since
 186 acidic values were measured at all conditions (pH = 2 - 3), the assumptions of fully protonated, non-
 187 ionic monomer and pH independent rate constants are quite accurate.

188 The applied model has been developed in a previous work[7]. The complete set of constitutive
 189 equations (material and population balances) is summarized in **Table S2** of SI, where **eq. S4-S9** are
 190 the material balances while the average molecular weight properties are evaluated through **eqs. S12**
 191 and **S14**. Note that it is also possible to evaluate the entire chain length distribution by solving the
 192 population balances **S11** and **S13** at selected chain length values. All these equations are applicable
 193 to the three reactor types under examination by proper adjustments.

194 **4. Results and discussion**

195 **4.1. Model validation**

196 The reliability of the model was assessed by simulating the experimental data from MAA
197 polymerization in batch, semibatch and continuous processes.

198 The three batch experiments reported in **Table 3** were examined first.

199

200 *Table 3 Experimental conditions of batch experiments.*

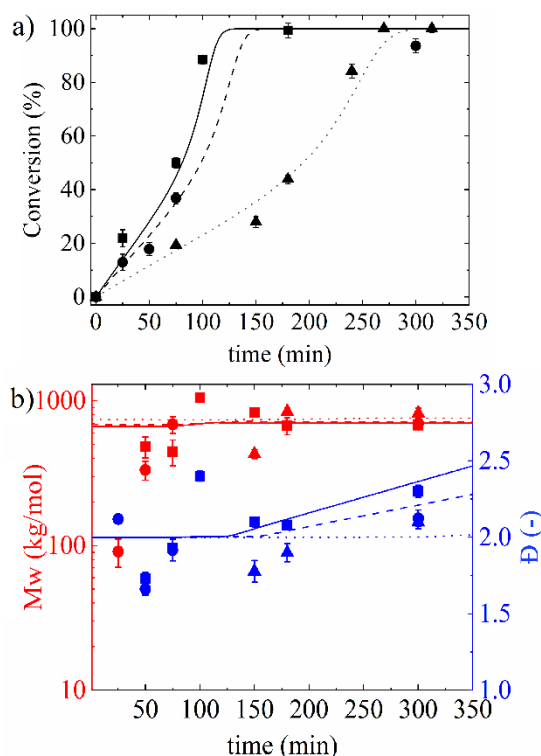
Experiment	Monomer [% w/w]	Initiator [% wbm]	T [°C]
1	5	0.5	50
2	5	2.0	50
3	5	3.0	50

201

202 The monomer conversion predicted by the model is compared with the experimental data in **Figure**
203 **1a**. Using the parameters reported in **Table 2** with a minor increase (*i.e.* 4x) in the value of $k_{tr,M}$, the
204 model predictions are quite in good agreement with the experiments, with deviations which are within
205 the experimental error (7%). The polymerization rate increases at increasing initiator concentration,
206 as expected, while auto-acceleration due to Trommsdorff effect is visible in all cases.

207 The experimental values of weight average molecular weight (Mw) and dispersity (\mathcal{D}) for the batch
208 experiments are depicted in **Figure 1b** along with the predictions provided by the model.

209



210

211 *Figure 1 Model vs. experimental conversion profile (a) and MWD (b). The curves (model) and the symbols (experimental data)*
 212 *reported represent the profiles of experiments 1 (... and ▲), 2 (--- and ●), and 3 (- and ■) in Table 3. The results shown are the*
 213 *average of three independent experiments with the error bars representing the standard deviation of the measurements.*

214

215 The experimental point at 25 min is definitely not reliable for this system. In fact, when a chain
 216 transfer to monomer mechanism is the dominant termination, the Mw is expected to be constant
 217 throughout the polymerization, as predicted by the model. This inaccuracy was attributed to the poor
 218 reliability of the analytics at low monomer conversion (< 30%). On the other hand, it is possible to
 219 appreciate the good predictivity of the model in terms of both Mw and Đ at higher monomer
 220 conversion.

221 Moving on to the semibatch configuration, the most popular operating mode in polymer industry, a
 222 wide range of operating conditions was simulated. Specifically, we selected low, intermediate, and
 223 high initiator concentration (*i.e.* from 1 to 3% wbm), feeding time between 20 and 120 minutes, and
 224 temperature between 50 and 60 °C. All the experimental conditions are summarised in **Table 4**.

225

226 *Table 4 Experimental conditions of semibatch experiments.*

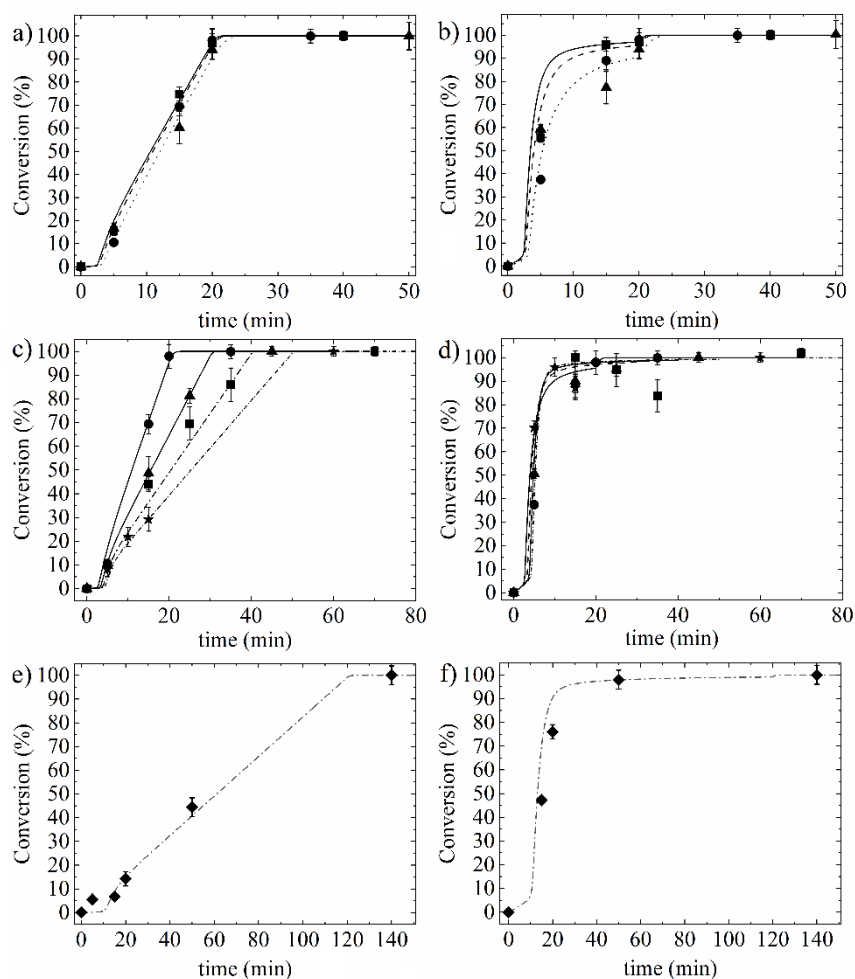
Experiment	Monomer [%]	Initiator [% wbm]	Temperature [°C]	Feeding time [min]
4	15	1	60	20
5	15	2	60	20
6	15	3	60	20
7	15	2	60	30

8	15	2	60	40
9	15	2	60	50
10	15	2	50	120

227

228 **Figures 2a, 2c and 2e** show the comparison between experimental and predicted monomer
 229 conversion. The instantaneous conversion values are reported in **Figures 2b, 2d and 2f**, defined as
 230 ratio between the produced polymer at time t and the monomer cumulatively fed to the reactor up to
 231 the same time t .

232



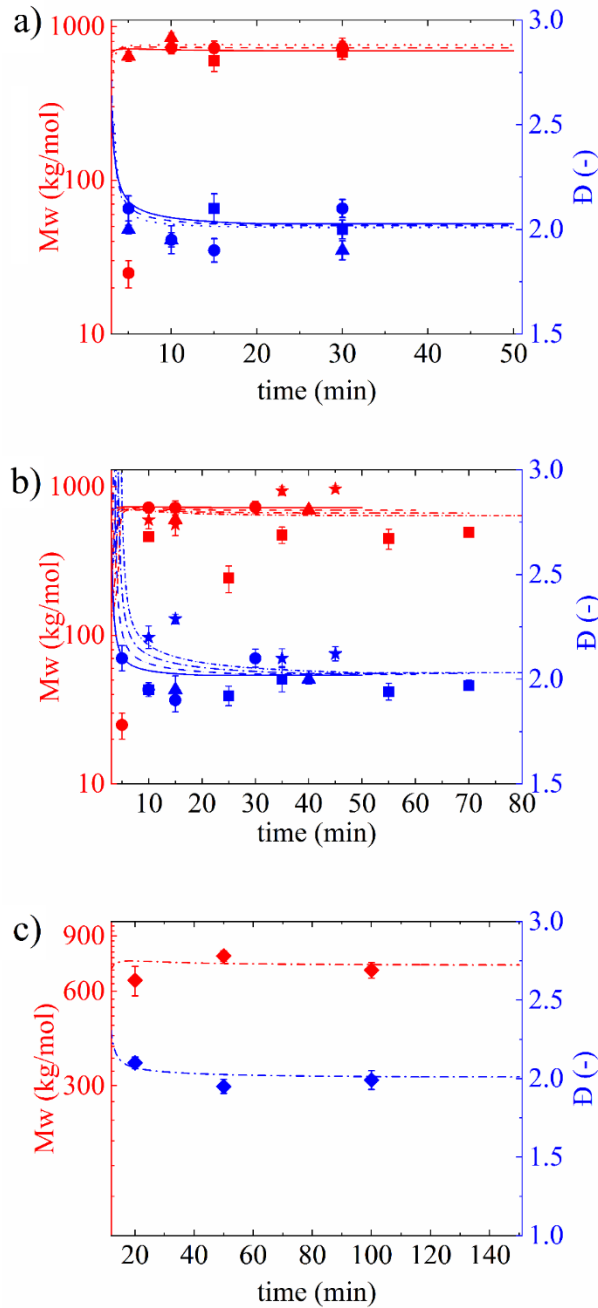
233

234 **Figure 2** Simulated vs. experimental cumulative (a, c, e) and instantaneous (b, d, f) conversion for semibatch reactor. In the case
 235 of (a, b) same FT (20 minutes) and initiator concentration equal to 1% wbm (... and ▲), 2% wbm (--- and ●), 3% wbm (- and ■).
 236 (c, d) same initiator concentration (2%) and FT equal to 20 (- and ●), 30 (--- and ▲), 40 (- . - and ■) and 50 minutes (-.- and ★).
 237 (e, f) FT 120 minutes. The curves are the model results, the symbols are the experimental results. The results shown are the
 238 average of three independent experiments with the error bars representing the standard deviation of the measurements.

239

240 A good agreement is obtained in all cases with the same parameter values previously applied for the
 241 batch case. The further reaction time of 30 minutes is effective to reach complete conversion in all
 242 cases, as verified also by the model.

243 The comparison model-experiment in terms of Mw and \bar{D} is shown in **Figure 3**. Again, the agreement
 244 is good when retaining the scaling factor 4x for $k_{tr,M}$ evaluated for the batch experiments (**Figure**
 245 **S2**). A moderate impact of the initiator concentration on the average chain length is verified.
 246



247
 248 *Figure 3 Model vs. experimental MWD average properties for semibatch reactor. (a) same FT (20 minutes) and initiator*
 249 *concentration equal to 1% wbm (... and \blacktriangle), 2% wbm (--- and \bullet), 3% wbm (- and \blacksquare), (b) same initiator concentration (2%) and FT*
 250 *equal to 20 (- and \bullet), 30 (--- and \blacktriangle), 40 (-.- and \blacksquare) and 50 minutes (-.- and \star), (c) FT 120 minutes. Curves are model*
 251 *simulations, symbols are experimental data. The results shown are the average of three independent experiments with the error*
 252 *bars representing the standard deviation of the measurements.*

253 Finally, the reliability of the model is verified in the case of a CSTR. Namely, four experiments are
 254 considered, whose recipe and operating conditions are reported in **Table 5**.

255

256 *Table 5 Experimental conditions of CSTR experiments*

Experiment	Inlet Monomer [M]	Inlet Water [M]	Inlet Initiator [% wbm]	Inlet Volumetric Flow Rate [L/min]	Temperature [°C]
11	1.84	46.74	5.5	$5 \cdot 10^{-3}$	60
12	1.82	46.86	2.0	$3 \cdot 10^{-3}$	60
13	1.80	46.93	5.5	$3 \cdot 10^{-3}$	60
14	1.78	47.01	1.0	$3 \cdot 10^{-3}$	60

257

258 In all cases, the model predicts the kinetic behaviour (**Figure 4a**) as well as the average MWD
 259 properties (**Figure 4b**) with acceptable accuracy. Note that all simulations have been carried out
 260 without any further parameter adjustment, thus supporting the prediction ability of the model. Given
 261 the wide range of reactor operating mode (from batch/semibatch to continuous) and explored
 262 conditions (monomer contents up to 15% w/w, initiator concentration in the range 0.5-5.5% wbm,
 263 and temperature between 50 and 60 °C), the model can be considered adequate to guide the transition
 264 from semi-continuous to continuous operations.

265

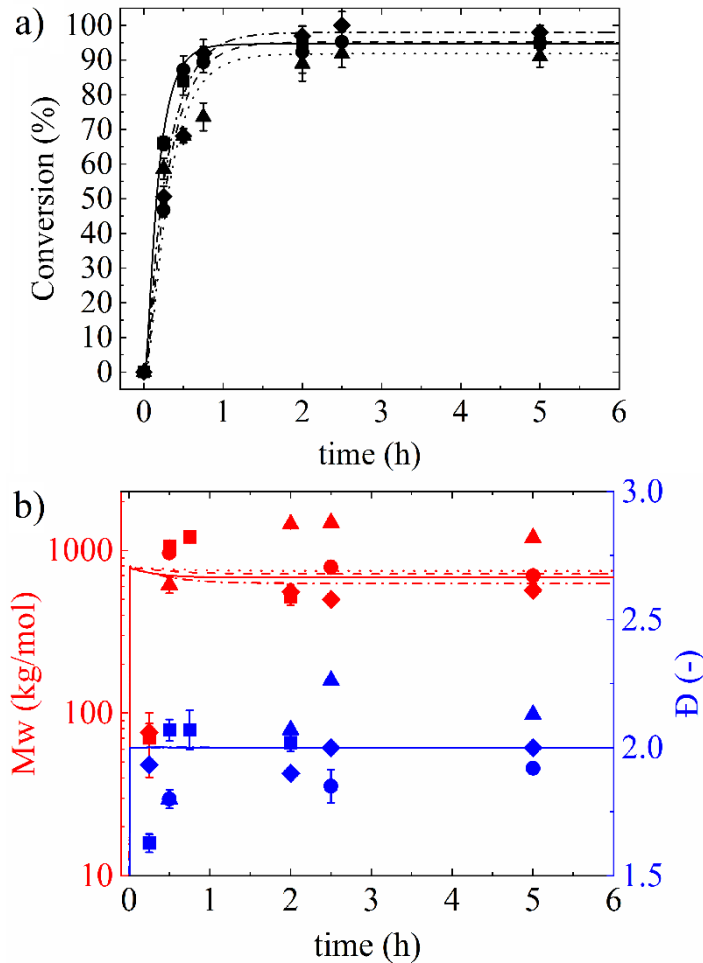


Figure 4 Model prediction vs. experimental conversion for the solution FRP of non-ionized MAA in a CSTR. The curves are model simulations, the symbols are experimental data. Conversion (a), Mw (b, red) and \bar{D} (b, blue) values for experiment 11 (- and ■), 12 (--- and ●), 13 (-. and ◆), and 14 (... and ▲) (cf. Table 5). The results shown are the average of three independent experiments with the error bars representing the standard deviation of the measurements.

4.2. Converting a semibatch production to continuous

Focusing on a well-established polymerization process carried out in semibatch, we now consider the design of the operating conditions of the equivalent reaction carried out in a CSTR while ensuring the same polymer quality (*i.e.* final PC of 15% w/w and final Mw of $6.9 \cdot 10^5$ g/mol). We considered a specific reactor volume (50 mL) to analyse the realistic situation where stirred reactors with constant volume are available (those previously used in batch or semibatch production) and have to be converted into continuous configurations. According to the semibatch process, the initiator concentration is 0.5% wbm, with 15% w/w of monomer fed in 120 minutes and 30 minutes of post-reaction (final batch stage). The process performances are 100% of conversion and a final productivity of $1 \cdot 10^{-3}$ g/min/mL considering 150 minutes as overall process duration. It is worth highlighting that this estimate is quite conservative since the actual productivity will be smaller. In

283 fact, a semibatch process is typically afflicted by considerable dead times (*i.e.* charging/discharging,
284 cleaning, and others).

285 Procedurally, we used the rigorous model equations in order to select the best operating conditions
286 able to reproduce in continuous the product obtained with the selected semibatch formulation. The
287 system composed by eqs. (S4)-(S10) and (S12) accounts for 10 equations. Given the absence of active
288 species (R_{in} and λ_1^{in}) and pre-formed polymer (P_{in} and $\mu_{j,in}$) fed to the reaction vessel, the number
289 of unknowns is equal to 15 and so 5 degrees of freedom need to be set. Given the reactor volume, we
290 defined an 11x2 matrix of reasonable values for the monomer and water inlet concentrations. Each
291 couple of values was readily calculated by considering the required PC and 11 hypothetical values of
292 monomer conversion in the range 95 - 100% (residual monomer smaller than 5% was considered) in
293 eq. (6):

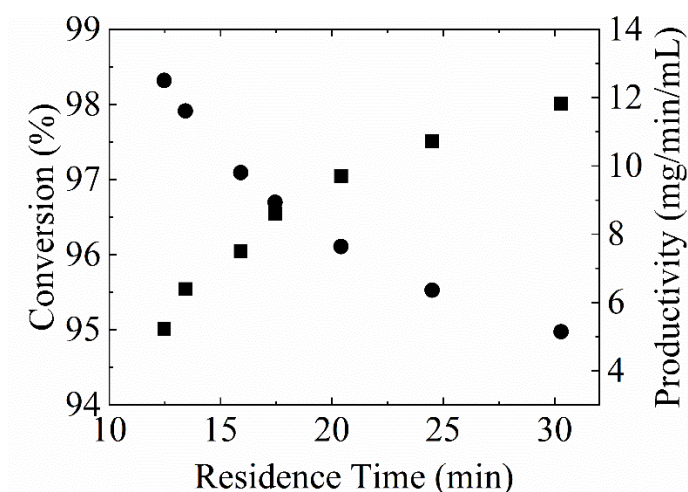
$$\chi = \frac{PC}{\%M_{in}} \cdot 100 \quad (6)$$

295

296 Thus, eq. (6) allows to obtain the mass percentage of monomer in the stream entering the reactor
297 ($\%M_{in}$) and, consequently, the corresponding molar concentration (M_{in}). Since the inlet stream is
298 only composed by monomer and water (initiator concentration can be neglected), the water
299 concentration entering the reactor (W_{in}) is readily evaluated.

300 Then, for each couple of monomer and water concentration, we arbitrarily varied the remaining
301 degrees of freedom, namely Q_{in} and I_{in} , in the range $2.08 \cdot 10^{-1}$ - 10 mL/min for Q_{in} (corresponding
302 to a mean residence time from a minimum value of 5 min to a maximum value of 240 min) and 0.1 -
303 6% wbm for the initiator. Namely, to scan all possible combinations inside the selected range of
304 values, a square calculus mesh of 30x30 has been applied, solving numerically the non-linear system
305 of model equations in their steady state version for each specific combination of Q_{in} and I_{in} . An
306 example of the model output in terms of PC and Mw obtained at conversion of 95% is shown in
307 **Figure S3**. The same approach was applied to each one of the 11 combinations water-monomer inlet
308 concentrations mentioned above, resulting in a set of PC and Mw surfaces fully equivalent to those
309 in the figure. The intersections between such surfaces and the planes representing the target values of
310 PC and Mw (blue planes in **Figure S3**) correspond to two curves, providing all pairs of values of Q_{in}
311 and I_{in} fulfilling one or the other target. At each specific conversion, the optimal values are finally
312 found as the intersection between these two curves, as summarized in **Table S3**. Notably, the values
313 in the table correspond to conversion values from 95 to 98%, since no solution is found at imposed
314 conversion values larger than 98%. These results are also shown in **Figure 5** in terms of conversion

315 and productivity as a function of the mean residence time: the expected trade-off between such two
316 quantities is found, since large residence times result in high conversions but low productivity.
317



318

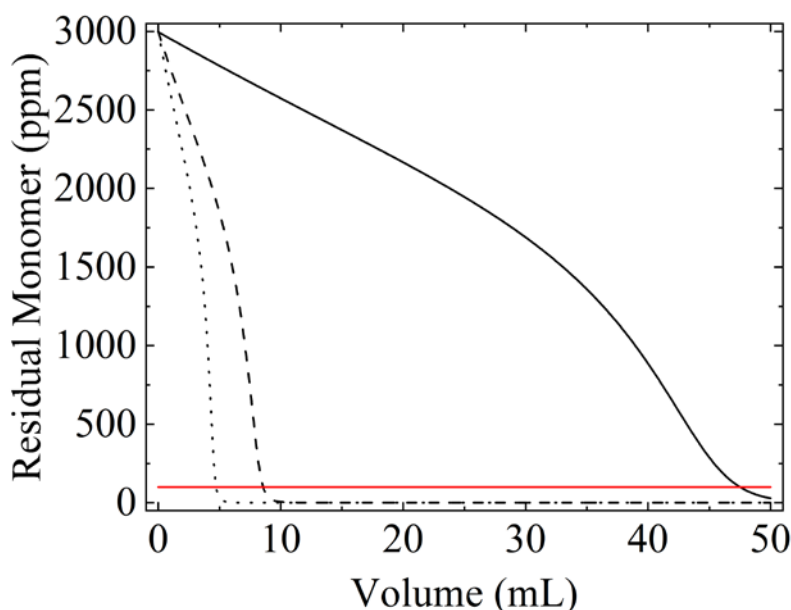
319 *Figure 5 Conversion (■) and productivity (●) vs. average residence time in a CSTR. Each symbol corresponds to specific values of*
320 *inlet monomer, water, and initiator concentrations, and inlet volumetric flow rate which guarantee the desired polymer content of*
321 *15% and weight-average molecular weight of $6.9 \cdot 10^5$ g/mol.*

322

323 Assuming maximum conversion (98%) as the strongest requirement, a productivity of $5.1 \cdot 10^{-3}$
324 g/min/mL is evaluated at mean residence time of 30.3 minutes, with a favourable productivity ratio
325 between CSTR and semibatch equal to 5.1. As expected, the produced polymer is fulfilling the
326 selected quality targets (polymer content and weight average molecular weight). On the other hand,
327 according to the dominant termination mechanism, its polydispersity is very close to 2 and the entire
328 molecular weight distribution is very close to that produced in the starved semibatch reactor, as shown
329 in **Figure S4**. Therefore, much higher productivity is obtained without affecting the product quality.
330 Nonetheless, very high conversions are of paramount importance in industry in order to minimize the
331 residual monomer. As a matter of fact, several strategies able to reduce the monomer content below
332 the limits imposed by the regulatory agencies are available. In the case of methacrylic acid the most
333 conservative critical threshold of residual monomer is 100 ppm[32]. An effective approach to
334 monomer depletion is the use of a short tubular reactor in series to the main CSTR. This unit ensures
335 the necessary reaction volume for reducing the monomer concentration at limited increase of fix costs
336 (usually its volume is small).

337 To simulate this reactor configuration, a plug flow reactor (PFR) in series to the CSTR was
338 considered, with inlet flow rate equal to the output flow rate of the CSTR along with the possible
339 increasing of the reaction temperature. The reaction mixture with final conversion equal to 98% is
340 considered as input to the PFR (see **Table S3**, entry 7). The residual monomer concentration as a

341 function of the reactor volume is reported in **Figure 6** for 3 reaction temperatures, *i.e.* 60, 80 and 90
342 °C.
343



344
345 *Figure 6 Residual monomer concentration vs. PFR volume. The curves represent different temperatures of the tubular reactor,*
346 *which increase as: 60°C (-), 80°C (- -), 90°C (..). The horizontal red line indicates a residual monomer equal to 100 ppm, set as*
347 *target.*

348
349 As expected, the PFR volume necessary to reduce the residual monomer concentration below the
350 critical value of 100 ppm (red line) depends on the reactor temperature. In particular, performing the
351 reaction at the same temperature of the CSTR (*i.e.* 60°C) leads to a large-volume PFR, very close to
352 the CSTR one (50 mL). Such reactor size would increase the total fix costs thus vanishing the
353 productivity improvement previously achieved with the CSTR configuration. On the other hand,
354 carrying out the reaction at higher temperatures dramatically reduces the tubular reactor volume up
355 to 5 mL at 90°C, as clearly shown in **Figure 6**, making this strategy appealing and economically
356 viable for the depletion of the residual monomer.
357 However, an increase in the reactor temperature in presence of unreacted monomer may alter the final
358 polymer properties since short chains are formed because of the very low monomer amount. For this
359 reason, we compared the MWD of the polymer leaving the PFR in the worst scenario (*i.e.* temperature
360 equal to 90°C) with the one of the polymer leaving the CSTR (see **Figure S5**). As can be seen from
361 the figure, no significant change in polymer MWD is observed. Moreover, considering to use an
362 empty tube with a diameter of 5 mm and a volume of 5 mL (the value necessary in the case of 90°C),
363 it is possible to calculate the length of the reactor that is equal to 25.5 cm. These small values coupled
364 with the fast monomer depletion and the preservation of polymer quality support the industrial
365 feasibility of the proposed process.

366 **5. Conclusions**

367 The transition from batch to continuous of non-ionized methacrylic acid free radical polymerization
368 has been explored taking advantage of a kinetic model of the polymerization reaction. The model
369 reliability has been confirmed by comparison between the model simulations and experimental data
370 collected in batch, semibatch as well as in continuous (CSTR) reactors. Then, the validated model
371 was applied to design the operating conditions suitable to convert a semibatch process into a
372 continuous one under the constraints of constant polymer quality (same average properties of
373 molecular weight) and same polymer content.

374 For a defined space of operating conditions, the maximum monomer conversion in the continuous
375 case is smaller than the complete conversion actually achieved in semibatch and equal to 98%. On
376 the other hand, a substantial improvement in the process productivity is found, with productivity ratio
377 between CSTR and semibatch equal to 5.1. In order to reduce to the minimum the residual monomer
378 in the final product, the use of a tubular reactor in series to the CSTR was also examined and modelled
379 through a PFR. Different monomer concentrations at the outlet of the tubular reactor can be achieved
380 on the basis of the given tubular reactor volume and reaction temperature.

381

382 **Supplementary Information**

383 Electronic supporting information are available at the publisher's website and include the
384 discretization of the outlet volumetric flow rate adopted for the CSTR model validation, the equations
385 used to evaluate the experimental conversion profiles in the three reactor configurations, the
386 mathematical model of the MAA solution polymerization process, the mathematical evaluation of the
387 formula that relates conversion, polymer content and inlet monomer concentration, the results of the
388 deterministic approach fixing a conversion of 95%, the recipes obtained through the basic
389 optimization procedure presented, the MWD of the products obtained from the selected semibatch
390 process and its conversion to a CSTR and the MWD of the products obtained from the selected CSTR
391 process and the one after the PFR.

392 **Conflicts of interest**

393 The authors report no competing interests for this work.

394

395 **Bibliography**

396 [1] P. Nesvadba, *Radical Polymerization in Industry*. 2012.

397 [2] J. Ilare and M. Sponchioni, "From batch to continuous free-radical polymerization: Recent

- 398 advances and hurdles along the industrial transfer,” *Adv. Chem. Eng.*, pp. 1–29, 2020, doi:
399 10.1016/bs.ache.2020.07.005.
- 400 [3] I. Rossetti and M. Compagnoni, “Chemical reaction engineering, process design and scale-up
401 issues at the frontier of synthesis: Flow chemistry,” *Chem. Eng. J.*, vol. 296, pp. 56–70, 2016,
402 doi: 10.1016/j.cej.2016.02.119.
- 403 [4] D. Kohlmann, M. Chevrel, S. Hoppe, D. Meimaroglou, D. Chapron, P. Bourson, C. Schwede,
404 W. Loth, A. Stammer, J. Wilson, P. Ferlin, L. Falk, S. Engell and A. Durand, “Modular,
405 Flexible, and Continuous Plant for Radical Polymerization in Aqueous Solution,” *Macromol.*
406 *React. Eng.*, vol. 10, no. 4, pp. 339–353, 2016, doi: 10.1002/mren.201500079.
- 407 [5] J. R. Richards and J. P. Congalidis, “Measurement and control of polymerization reactors,”
408 *Comput. Chem. Eng.*, vol. 30, no. 10–12, pp. 1447–1463, 2006, doi:
409 10.1016/j.compchemeng.2006.05.021.
- 410 [6] M.-C. Chevrel, S. Hoppe, D. Meimaroglou, L. Falk, and A. Durand, “Continuous Pilot-Scale
411 Tubular Reactor for Acrylic Acid Polymerization in Solution Designed Using Lab-Scale Rheo-
412 Raman data,” *Macromol. React. Eng.*, vol. 10, no. 4, pp. 354–363, 2016, doi:
413 10.1002/mren.201500058.
- 414 [7] J. Ilare, M. Sponchioni, G. Storti, and D. Moscatelli, “From batch to continuous free-radical
415 solution polymerization of acrylic acid using a stirred tank reactor,” *React. Chem. Eng.*, vol.
416 5, no. 11, pp. 2081–2090, 2020, doi: 10.1039/D0RE00252F.
- 417 [8] S. Fathi Roudsari, F. Ein-Mozaffari, and R. Dhib, “Use of CFD in modeling MMA solution
418 polymerization in a CSTR,” *Chem. Eng. J.*, vol. 219, pp. 429–442, 2013, doi:
419 10.1016/j.cej.2012.12.049.
- 420 [9] A. Durand and S. Engell, “Batch to Conti Transfer of Polymer Production Processes,”
421 *Macromol. React. Eng.*, vol. 10, no. 4, pp. 308–310, 2016, doi: 10.1002/mren.201600031.
- 422 [10] C. Schoppmeyer, H. Vermue, S. Subbiah, D. Kohlmann, P. Ferlin, and S. Engell, “Operation
423 of Flexible Multiproduct Modular Continuous Polymerization Plants,” *Macromol. React. Eng.*,
424 vol. 10, no. 4, pp. 435–457, 2016, doi: 10.1002/mren.201500044.
- 425 [11] G. Montesissa, A. Olivieri, and G. Scapellato, “Alkyd resins modified with acrylic or
426 methacrylic acid for use in water based paints,” US3894978A, 1975.
- 427 [12] A. K. Khan, B. C. Ray, and S. K. Dolui, “Preparation of core-shell emulsion polymer and

- 428 optimization of shell composition with respect to opacity of paint film,” *Prog. Org. Coatings*,
429 vol. 62, no. 1, pp. 65–70, 2008, doi: 10.1016/j.porgcoat.2007.09.022.
- 430 [13] C. E. Frank, G. Kraus, and A. J. Haefner, “Butadiene–Methacrylic Acid Copolymers as
431 Rubber-to-Steel Adhesives,” *Ind. Eng. Chem.*, vol. 44, no. 7, pp. 1600–1603, 1952, doi:
432 10.1021/ie50511a033.
- 433 [14] B. Loomans, N. Opdam, T. Attin, D. Bartlett, D. Edelhoff, R. Frankenberger, G. Benic, S.
434 Ramseyer, P. Wetselaar, B. Sterenborg, R. Hickel, U. Pallesen, S. Mehta, S. Banerji, A. Lussi
435 and N. Wilson, “Severe Tooth Wear: European Consensus Statement on Management
436 Guidelines,” *The Journal of Adhesive Dentistry*, vol. 19, no. 2, pp. 111–119, 2017, doi:
437 10.3290/j.jad.a38102.
- 438 [15] S. N. Jaisankar, S. Ramalingam, H. Subraman, R. Mohan, P. Saravanan, D. Samanta and A.
439 Mandal “Cloisite-G-methacrylic acid copolymer nanocomposites by graft from method for
440 leather processing,” *Ind. Eng. Chem. Res.*, vol. 52, no. 4, pp. 1379–1387, 2013, doi:
441 10.1021/ie300290g.
- 442 [16] B. Saha and M. M. Sharma, “Esterification of formic acid, acrylic acid and methacrylic acid
443 with cyclohexene in batch and distillation column reactors: Ion-exchange resins as catalysts,”
444 *React. Funct. Polym.*, vol. 28, no. 3, pp. 263–278, 1996, doi: 10.1016/1381-5148(95)00092-5.
- 445 [17] S. Alay Aksoy, C. Alkan, M. S. Tözüm, S. Demirbağ, R. Altun Anayurt, and Y. Ulcay,
446 “Preparation and textile application of poly(methyl methacrylate-co-methacrylic acid)/n-
447 octadecane and n-eicosane microcapsules,” *J. Text. Inst.*, vol. 108, no. 1, pp. 30–41, 2017, doi:
448 10.1080/00405000.2015.1133128.
- 449 [18] S. B. Vitta, E. P. Stahel, and V. T. Stannett, “The Preparation and Properties of Acrylic and
450 Methacrylic Acid Grafted Cellulose Prepared by Ceric Ion Initiation. Part I. Preparation of the
451 Grafted Cellulose,” *J. Macromol. Sci. Part A - Chem.*, vol. 22, no. 5–7, pp. 579–590, 1985,
452 doi: 10.1080/00222338508056624.
- 453 [19] M. Buback, P. Hesse, R. Hutchinson, P. Kasa, I. Laci, M. Stach, and I. Utz, “Kinetics and
454 modeling of free-radical batch polymerization of nonionized methacrylic acid in aqueous
455 solution,” *Ind. Eng. Chem. Res.*, vol. 47, no. 21, pp. 8197–8204, 2008, doi: 10.1021/ie800887v.
- 456 [20] S. Beuermann, M. Buback, P. Hesse, R. A. Hutchinson, and I. Laci, “Termination Kinetics of
457 the Free-Radical Polymerization of Nonionized Methacrylic Acid in Aqueous Solution,” pp.
458 3513–3520, 2008.

- 459 [21] S. Beuermann, M. Buback, P. Hesse, and S. Kukuc, "Propagation Rate Coefficient of Non-
460 ionized Methacrylic Acid Radical Polymerization in Aqueous Solution . The Effect of
461 Monomer Conversion," pp. 41–49, 2007, doi: 10.1002/masy.200750205.
- 462 [22] E. J. Fischer, G. Storti, and D. Cuccato, "Aqueous Free-Radical Polymerization of Non-Ionized
463 and Fully Ionized Methacrylic Acid," *Processes*, vol. 5, 2017, doi: 10.3390/pr5020023.
- 464 [23] Y. J. Katsuhiko, Iwase, Kazunori Miyuki, Sasaki Keigo, Watanabe Harumi, "METHOD FOR
465 PRODUCING METHACRYLIC RESIN," JP2018035225A, 2016.
- 466 [24] H. Junichi Yoshida, K. Watanabe, and M. K. Iwase, Keigo Sasaki, "METHACRYLIC
467 RESIN," US 10174145 B1, 2019.
- 468 [25] S. Beuermann, M. Buback, P. Hesse, and I. Lacík, "Free-radical propagation rate coefficient
469 of nonionized methacrylic acid in aqueous solution from low monomer concentrations to bulk
470 polymerization," *Macromolecules*, vol. 39, no. 1, pp. 184–193, 2006, doi: 10.1021/ma051954i.
- 471 [26] S. Beuermann, M. Buback, P. Hesse, R. A. Hutchinson, S. Kukučková, and I. Lacík,
472 "Termination kinetics of the free-radical polymerization of nonionized methacrylic acid in
473 aqueous solution," *Macromolecules*, vol. 41, no. 10, pp. 3513–3520, 2008, doi:
474 10.1021/ma7028902.
- 475 [27] N. Manfredini J. Ilare, M. Invernizzi, E. Polvara D. Contreras Mejia, S. Sironi, D. Moscatelli
476 and M. Sponchioni, "Polymer nanoparticles for the release of fragrances: How the physico-
477 chemical properties influence the adsorption on textile and the delivery of limonene," *Ind. Eng.*
478 *Chem. Res.*, 2020, doi: 10.1021/acs.iecr.0c02075.
- 479 [28] J. E. Mark, "Polymer data handbook," *Oxford Univ. Press*, 1999.
- 480 [29] C. Costa, A. Alberton, A. Santos, M. Fortuny, P. Araújo, C. Sayer and J. Pinto,, "Kinetic
481 Parameters of the Initiator Decomposition in Microwave and in Conventional Batch Reactors
482 - KPS and V50-Case Studies," *Macromol. React. Eng.*, vol. 9, no. 4, pp. 366–373, 2015, doi:
483 10.1002/mren.201500013.
- 484 [30] J. Barth and M. Buback, "SP-PLP-EPR study into the termination kinetics of methacrylic acid
485 radical polymerization in aqueous solution," *Macromolecules*, vol. 44, no. 6, pp. 1292–1297,
486 2011, doi: 10.1021/ma102278n.
- 487 [31] N. F. G. Wittenberg, M. Buback, and R. A. Hutchinson, "Kinetics and Modeling of
488 Methacrylic Acid Radical Polymerization in Aqueous Solution," *Macromol. React. Eng.*, vol.

489 7, no. 6, pp. 267–276, Jun. 2013, doi: 10.1002/mren.201200089.

490 [32] E. Commission, “European Union Risk Assessment Report,” 2002. [Online]. Available:
491 <https://echa.europa.eu/documents/10162/f0b94b4b-a87b-442b-b647-8ff56895c92c>.

492

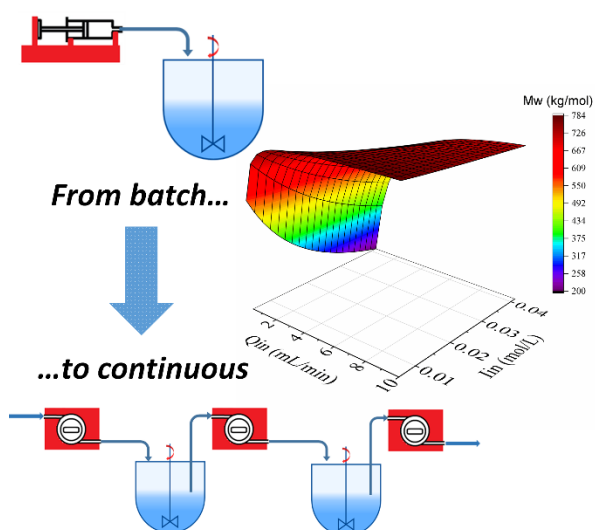
Table of Contents for Free-Radical Polymerization of Methacrylic Acid: From Batch to Continuous Using Stirred Tank Reactors

Juri Ilare^{1,#}, Nicolò Manfredini^{1,#}, Mattia Sponchioni^{1,}, Giuseppe Storti¹ and Davide Moscatelli¹*

¹ Department of Chemistry, Materials and Chemical Engineering, Politecnico di Milano, Via Mancinelli 7, 20131 Milano, Italy.

[#]Jl and NM equally contributed to the work

*corresponding author: Mattia Sponchioni, e-mail: mattia.sponchioni@polimi.it



Model-assisted optimization to convert a semibatch poly(methacrylic acid) production to continuous preserving the same average molecular weight and dry content.